The Journal of the Oceanological Society of Korea
Vol. 19, No. 1, p. 24-30, June 1984.

A Numerical Experiment of the Effect of Coastline Geometry on the Upwelling along the East Coast of Korea

Young Ho Seung
Dept. of Oceanography, Inha University, Incheon, 160

韓國東岸 沿岸線形態가 湧昇에 미치는 影響에 관한 數値實驗

承 永 鎬
仁荷大 海洋學科

Abstract: A numerical experiment was carried out on the wind-induced coastal upwelling along the east coast of Korea. Only the variability in coastline geometry is considered and an attempt is made to correlate it with the observation previously performed. In order to approximate the coastline geometry as closely as possible, the finite element method with linear triangular grid is employed. Among several fixed locations of upwelling center found in the model, the one in the southeastern coastal area seems to be just what has been observed most frequently.

要約: 한국 동해안을 대상으로하여 바람에 의한 湧昇을 數値실험을 통하여 관찰하였다. 本考에서는 연안선의 형태에 따르는 효과만을 고찰하였으며 실제로 東海岸에서 관측되어온 결과와 결부시키려고 하였다. 실제와 近似한 연안선을 보다 효율적으로 만들기 위하여 有限要素法을 도입하였다. 실험결과 몇개의 湧昇域이 發見되었으며 그중 한개는 東南海域에서 자주 관측되어온 冷水域임이 밝혀졌다.

INTRODUCTION

Along the southeast coast of Korea, the cold surface water has been frequently observed during the summer(An, 1974; Seung, 1974; Lee, 1983) as shown in Fig. 1. Many explanations have been given to this phenomenon. Kim and Kim(1983) reported that this cold surface water is an extension of the North Korea Cold Current which flows southward along the coast. The shoaling of deep cold water toward the coast, caused by the strengthening of the northward bound Tsushima Warm Current, may also contribute to this phenomena (Seung, 1974). On the other hand, Lee(1978) emphasized the significance of the cyclonic circulation of the Tsushima Current in this area. Seung(1974) and Lee(1983) conjectured the important role of the local wind which induces the coastal upwelling. In particular, Lee(1983) showed a significant correlation among sea level, surface temperature and southwesterly wind blowing parallel to the coastline.

A remarkable feature is that the coldest water appears often at fixed locations along the line joining Ulsan and Gampo(Fig. 1) which, otherwise, should propagate along the coastline as an internal Kelvin wave. There should be many unknown factors involved in this phenomenon. However, in this paper, an attempt is made to correlate their fixed locations with the coastline geometry alone, which implies a variability in the local alongshore component of large scale wind stress field.

In order to approximate the coastline geometry as closely as possible, a numerical finite element using a linear triangular grid is chosen. The employed numerical scheme is very simple (Seung and Lee, 1984) and it retains an unco-

Manuscript received 9 April 1984.

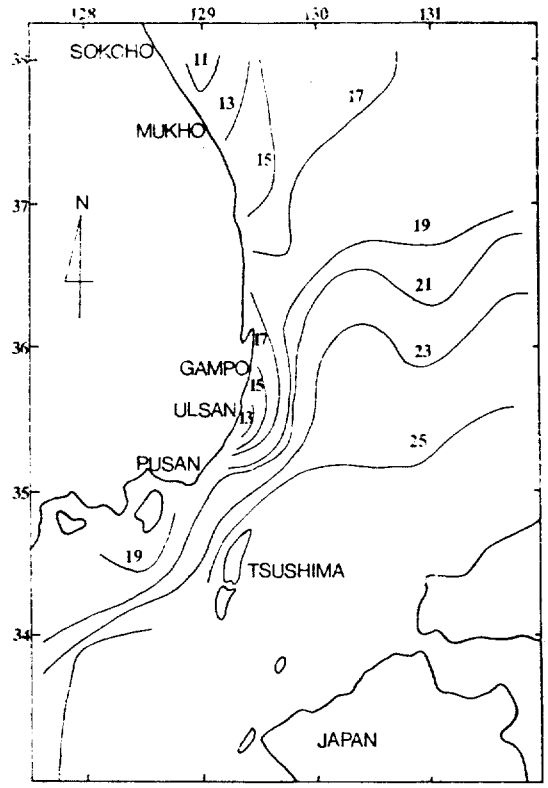

Fig. 1. Temperature distribution in degree centigrade at 20m depth in August 1967 and 1968 averaged over the years, extracted from Seung (1974).

nditional stability of the system.

GOVERNING EQUATIONS

The vertical variation of density may be approximated assuming a homogeneous two layer fluids. Hydrostatic and Boussinesq assumptions employed and the equations are vertically integrated in each layer. Assuming small perturbations from rest, the equations can be linearized. The resulting equations are:

in the upper layer

$$\frac{\partial \boldsymbol{u}_1}{\partial t}+f\boldsymbol{k}\times\boldsymbol{u}_1=-gh_1\nabla\xi_1+\tau/\rho_1 \tag{1}$$

$$\frac{\partial}{\partial t}(\xi_1-\xi_2)+\nabla\cdot\boldsymbol{u}_1=0 \tag{2}$$

in the lower layer

$$\frac{\partial \boldsymbol{u}_2}{\partial t}+f\boldsymbol{k}\times\boldsymbol{u}_2=-gh_2\nabla\xi_2+gh_2\varepsilon\nabla(\xi_1-\xi_2) \tag{3}$$

$$\frac{\partial \xi_2}{\partial t}+\nabla\cdot\boldsymbol{u}_2=0 \tag{4}$$

where

$\xi_1(\xi_2)$ elevation of the sea surface (interface) from rest

$\boldsymbol{u}_1(\boldsymbol{u}_2)$ vertically-integrated velocity in the upper (lower) layer

g gravity constant

$\boldsymbol{k}$ unit vector positive upward in the vertical axis

$h_1(h_2)$ thickness of the upper (lower) layer at rest

ρ_1 density of the upper layer

ε density ratio

τ wind stress vector at the sea surface

The stress at the interface is small and can be neglected. Therefore, the coupling between the upper and lower layers is due only to the pressure forces. The total depth (h_1+h_2) is held constant since the effect of bottom topography is not considered here. The bottom stress is assumed insignificant. Since the scale of considered motion is not large, the beta-effect is also neglected.

Using a technique described by Csanady (1975), equations (1) through (4) can be separated into two independent ones which are mathematically equivalent. In fact, the resulting two equations represent the surface and internal mode which are expressed as follows:

surface mode

$$\frac{\partial}{\partial t}(\boldsymbol{u}_1+\boldsymbol{u}_2)+f\boldsymbol{k}\times(\boldsymbol{u}_1+\boldsymbol{u}_2)=-g(h_1+h_2)\nabla\xi_1-\tau/\rho_1 \tag{5}$$

$$\frac{\partial \xi_1}{\partial t}+\nabla\cdot(\boldsymbol{u}_1+\boldsymbol{u}_2)=0 \tag{6}$$

internal mode

$$\frac{\partial \boldsymbol{u}_2}{\partial t}+f\boldsymbol{k}\times\boldsymbol{u}_2=-g\varepsilon\frac{h_1h_2}{h_1+h_2}\nabla\xi_2-\frac{h_2}{h_1+h_2}\tau/\rho_1 \tag{7}$$

$$\frac{\partial \xi_2}{\partial t}+\nabla\cdot\boldsymbol{u}_2=0 \tag{8}$$

These equations were solved analytically by Csanady (1975) for two-dimensional problem, and by Crepon for three-dimensional problem.

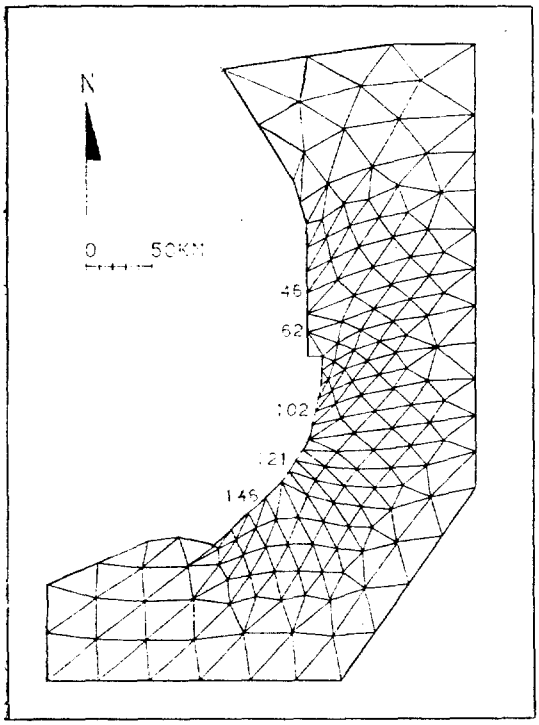

Fig. 2. Finite element grid of the study area. Five nodes are numbered where the interface elevations are recorded continously during the experiment.

In three-dimensional problem, the Kelvin waves are generated at discontinuities in alongshore component of wind stress, and then propagate along the coastline. The response to the wind can be divided into two classes according as wheather the wind field is divergent or rotational. For divergent field, the disturbance soon becomes independent of time. Whereas, for the rotational field, it increases indefinitely with time unless the Kelvin wave fronts arrive. In this paper, we aim to solve the equations (5) through (8) for relatively uniform southwesterly wind blowing over a large oceanic area with realistic coastline geometry.

NUMERICAL EXPERIMENT

The grid used for the realistic simulation of the eastern coastal waters of Korea is shown in Fig. 2. It has a total of 287 triangles. The smallest resolution is about 7.5km in the region of interest and the largest one is about 50km around the outer boundaries. A uniform and constant wind force is imposed suddenly at time $t=0$ over the domain which was initially at rest. The outer boundaries are established artificially to avoid the long computing time. No flux condition is imposed along these boundaries as well as along the coastline. The real conditions may then be affected by Kelvin waves generated along these boundaries and then entering into the region of interest. Otherwise, the effect of these boundaries would extend no farther than the deformation radius(r) from these boundaries(Hua, 1981). Table 1 summarizes all physical parameters employed in our experiment. These values are chosen to be as realistic as possible to the observed ones(for example Kim and Kim, 1983). Referring to Table 1, it can be realized that the internal mode has relatively small propagation speed($c=\sqrt{g\varepsilon\frac{h_1h_2}{h_1+h_2}}=54$km/day) and small scale of motion ($r=c/f=6.3$km). On the other hand, the external mode has relatively large propagation speed($c=\sqrt{g(h_1+h_2)}=3,024$ km/day) and large scale of motion($r=c/f=350$ km). Therefore, the solution for the internal mode can be obtained within 3~4days from the initial state since the waves generated at artificial boundaries takes 3~4days to propagate into the region of interest. As for the external mode, solutions are prone to errors and will not

Table 1. Values of physical parameters employed in the model

parameter	symbol	value
Coriolis' parameter	f	8.133×10^{-5}sec^{-1}
wind stress	τ_x	$0.049N/m^2$
	τ_y	$0.010N/m^2$
upper layer depth	h_1	25m
lower layer depth	h_2	100m
density ratio	ε	0.002
gravity constant	g	9.8m/sec^2

be considered hereafter. Note that the elevation of interface(ξ_2) is determined mostly by the internal mode. i.e. equations (7) and (8).

RESULTS

The time evolution of computed interface elevation(Fig. 3) recorded at arbitrarily chosen five node points(refer to Fig. 2 for position) shows that the inertial oscillation is of minor importance in upwelling problem. The contour maps of elevation are made for 6 different instants(Fig. 4) and they show the spatial distribution of upwelling. For the sake of convenience, reference positions are marked by the letters from A through E. These positions indicate the regions where relatively intense upwelling occurs throughout the experiment.

Generally, the location of upwelling center is well defined. The upwelling centers can be clearly seen at C and D soon after the wind starts to blow. At other locations, i.e. at A, B and E, they become distinctive in about one day. In

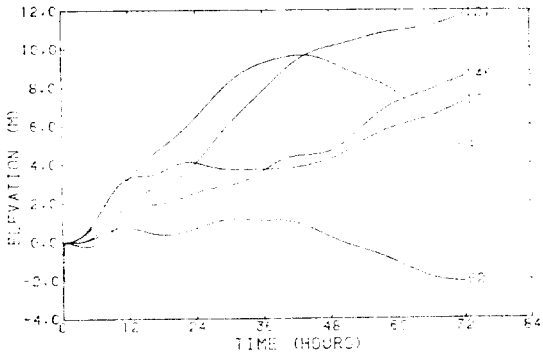

Fig. 3. Evolution of the computed interface elevation recorded at arbitrarily chosen 5 nodes (refer to Fig. 2).

the southern part, the upwelling area slowly extends to the south. This may be due to the effect of internal Kelvin wave propagation. Same effect can be seen in the northern part at an early stage. However, the propagation seems to be blocked soon by the abrupt change in coastline geometry especially at C. The estimated speed of propagation is slightly smaller than 50km/day, which is to be expected on the

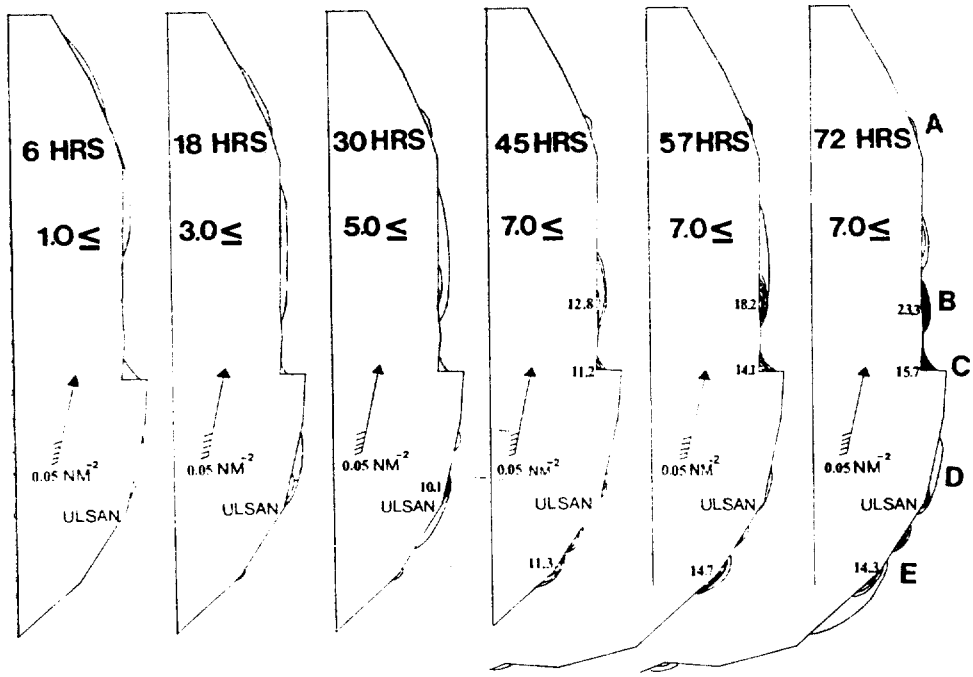

Fig. 4. Cotour maps of interface elevation at 6 different instants. Contourings are made at every 2m interval starting from 1, 3, 5 and 7m following the development of upwelling. Some of local maxima are shown in meter. The reference positions are maked by the letters from A through E. Also marked is the wind stress by an arrow.

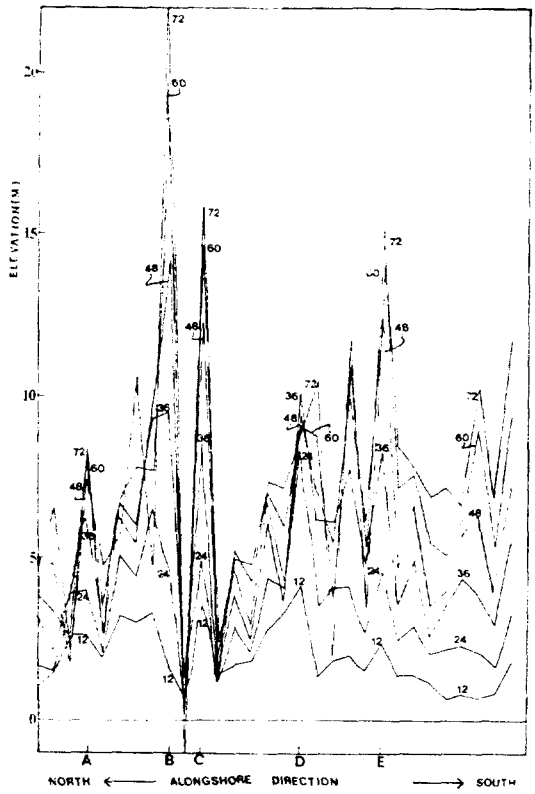

Fig. 5. Interface elevations at the coast plotted as a function of alongshore position at every 12 hour interval. Times are marked in hour along the curves.

straight coastline. The evolution of coastal upwelling may be seen more easily in Fig. 5 where the interface elevations at the coast are plotted as a function of alongshore position at every 12 hour interval. The rate of intensification of upwelling is very high at B and C whereas it is low at A. At D, the upwelling grows relatively fast during the first 36 hours. However, it becomes stagnant after then. On the other hand, at E, it is initially indistinct but, after 36 hours, it grows rapidly until finally it becomes more intense than that at D.

Fig. 6 shows the computed current in lower layer. It suggests that the coastal undercurrent may well develop in this area It is confined

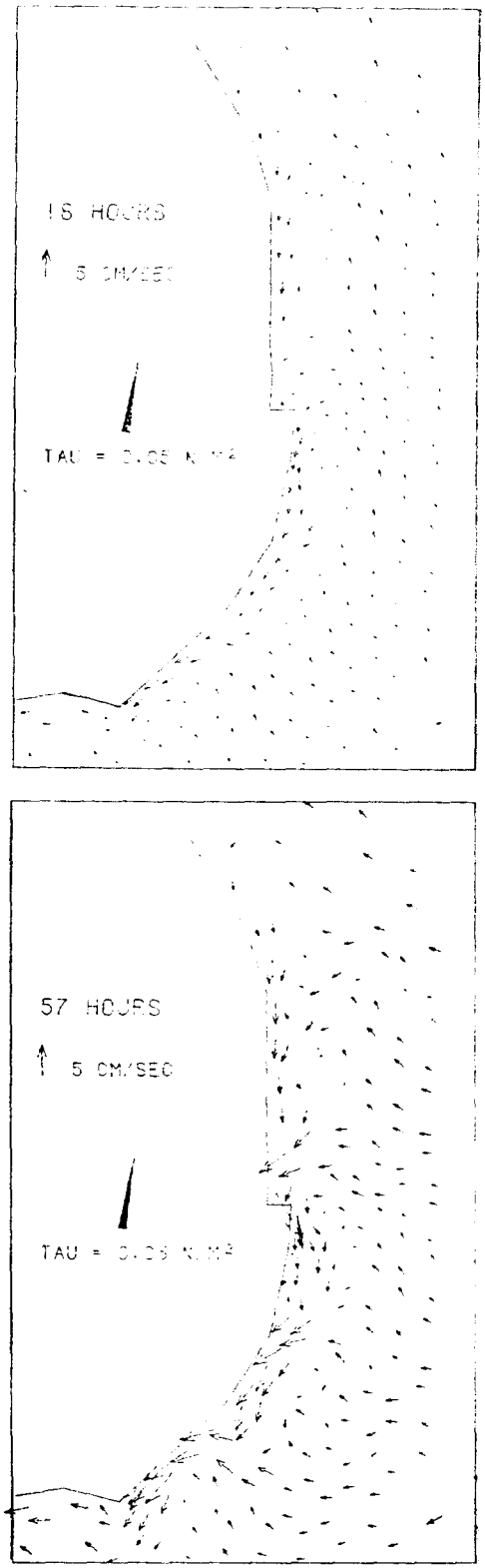

Fig. 6. Computed currents for the internal mode in lower layer at two different instants. →

within the narrow coastal region of which the width is comparable to the deformation radius (r). The formation of undercurrent implies that there is an alongshore variation of pressure field which is induced by the variability in the local alongshore component of wind stress. Similar effect has once been observed in this area by Seung and Byun(1984). In the offshore region, the onshore transport predominates to compensate the offshore Ekman drift in the upper layer.

CONCLUDING REMARKS

Application of simple, but essential, physical law to an area with realistic geometry may be meaningful in itself. The results obtained in this way verified the fact that there can exist some fixed locations where the upwelling is most favorable. The upwelling area known to be most frequently observed is the coastal zone between Ulsan and Gampo (Fig. 1). This is just around D in Fig. 4. However, according to the results of this study, even more intense upwelling can occur at other locations, especially near B and C in the north and near E in the south. This discrepancy may be due to other factors such as advection predominating over the effect of wind in the north.

This model may be too simple to be realistic since only the variability in coastline geometry is considered. Inclusion of bottom topography, non-linear effect, interactions with other components, and also the turbulent mixing between upper warmer and lower colder waters may result in more complete feature. Hua and Thomasset (1983) have performed nearly the same experiment for the coastal upwelling in the Gulf of Lions. They stressed the important role of mixing which reduces the propagation speed of the Kelvin wave fronts and allows the centers to persist and to spread out. In this paper, the inclusion of mixing would produce a better result, for the upwelling centers keep their initial position and the formation of new upwelling area is much restrained especially in the south, i.e. near D and E.

ACKNOWLEDGEMENT

The author gratefully acknowledges the '83 financial support given to this work by the Ministry of Education. The research subject was originally entitled as "Numerical modeling of wind-induced coastal trapped waves by using the Finite Element Method" when proposed. He also would like to thank Dr. S.R. Lee of KORDI for his kind cooperation in data generation and computer plotting.

REFERENCES

An, H.S., 1974. On the cold water mass around the southeast coast of Korean peninsula. J. Oceanol. Soc. Korea, 9:10-18.

Crepon, M. and C. Richez, 1982. Transient upwelling generated by two-dimensional atmospheric forcing and variability in the coastline. J. Phys. Oceanogr., 12:1437-1457.

Csanady, G.T., 1975. The coastal jet conceptual model in the dynamics of shallow seas. In: The sea, ideas and observations on progress in the study of the seas, Vol. 6, Marine modeling. Ed. Goldberg, E et al., Wiley: 117-144.

Hua, B.L., 1981. Modelisation numerique d'upwellings cotiers a l'aide d'une methode d'elements finis. Application au Golfe du Lion. These Doct. es Sciences, Univ. Paris 6.

Hua, B.L. and F. Thomasset, 1983. A numerical study of the effects of coastline geometry on wind-induced upwelling in the Gulf of Lions. J. Phys. Oceanogr., 13:678-694.

Kim, C.H. and K. Kim, 1983. Characteristics and origin of the cold water mass along the east coast of Korea. J. Oceanol. Soc. Korea, 18:73-83 (in Korean).

Lee, J.C., 1983. Variations of sea level and sea surface temperature associated with wind-induced upwelling in the southeast coast of Korea in summer.

J. Oceanol. Soc. Korea, 18:149-160.

Lee, K.B., 1978. Study on the coastal cold water near Ulsan. J. Oceanol. Soc. Korea, 13:5-10.

Seung, Y.H., 1974. A dynamic consideration on the temperature distribution in the east coast of Korea in August. J. Oceanol. Soc. Korea, 9:52-58 (in Korean).

Seung, Y.H. and S.K. Byun, 1984. Measurements of storm-generated baroclinic motions along the east coast of south Korea. In: Ocean Dynamics of Japan and East China Seas. Ed. Ichiye, T., Elsevier Oceanographic Series, Elsevier Publ., Amsterdam. (in press)

Seung, Y.H. and S.R. Lee, 1984. A numerical experiment of tide in Jinhae Bay by the finite element method. Bull. Korea Ocean Res. Dev. Inst. (in Korean) (in press).